Journal of Environmental Chemical Engineering 13 (2025) 118098

Contents lists available at ScienceDirect

Journal of Environmental Chemical Engineering

journal homepage: www.elsevier.com/locate/jece

Shielding the environment: Perfluoroalkylated pyrenes prevent lead leakage from perovskite solar cell

Silvia Orecchio [a], Diana Amorello [b], Annalinda Contino [c], Giuseppe Maccarrone [c], Alessandro Giuffrida [c], Santino Orecchio [b], Tiziana Fiore [a], Ivana Pibiri [b], Davide Ricci [b], Bruno Pignataro [a], Salvatore Barreca [c,*], Giuseppe Arrabito [a]

[a] Department of Physics and Chemistry "E. Segrè", University of Palermo, Viale Delle Scienze. Ed. 17, Palermo 90100, Italy
[b] Department of Biological, Chemical and Pharmaceutical Sciences and Technologies, University of Palermo, Viale Delle Scienze. Ed. 17, Palermo 90100, Italy
[c] Department of Chemical Sciences, University of Catania, Viale Andrea Doria 6, Catania 95125, Italy

ARTICLE INFO

Keywords:
Lead leaching from solar cells
Standard procedures in leaching solar cells
New materials in perovskite

ABSTRACT

Lead leaching from perovskite solar cells remains a critical environmental concern, particularly in humid conditions that accelerate degradation. This study investigates the role of perfluorinated pyrene compounds in the Hole Transport Layer (HTL) as a promising strategy to reduce lead release from perovskite solar cells. For the first time, at the best of our knowledge, the tests were carried out by using the normalized condition dictated by standard UNI EN 12457–2. The Atomic Force Microscopy analyses reveal that the incorporation of perfluoroalkylated pyrene compounds reduced surface roughness and enhanced film uniformity, thereby preventing lithium salt aggregation and maintaining the structural integrity of the HTL without significantly altering the efficiency of the photovoltaic device. Moreover, a decrease in lead leaching was observed, from 5.5 to 3.0 mg/L, in the photovoltaic modules when Perfluoroalkylated Pyrenes were added. Furthermore, the hydrophobic nature of these compounds significantly limits lead leaching, by approximately 45 %, compared to conventional perovskite solar cells. As a result, the addition of perfluoroalkylated pyrene compounds effectively decreases lead leaching, contributing to improved environmental stability and device longevity. These findings highlight a promising strategy for reducing lead contamination in perovskite photovoltaics, paving the way for more sustainable and stable solar cell technologies.

1. Introduction

Nowadays, in all countries, most of electricity is produced using fossil fuels, which are well known to be non-renewable energy sources [1]. Their combustion produces greenhouse gases (CO_2, CH_4, N_2O, etc.) that cause global temperatures to rise by approximately 1.5 °C since 1850 [2] and, due to incomplete combustion [3] release of hazardous pollutants, as well as solid waste (ashes). Thus, there is a growing demand for renewable energy sources, among which, in the industrial and research fields, photovoltaics plays a prominent role, due to the particularly favourable ratio between costs and effectiveness. Today, researchers and several industrial companies are studying organic solar cells (OSCs) and perovskite solar cells (PSCs) [4], with the aim of obtaining higher efficiencies compared to conventional silicon solar cells, using new materials as light absorbers. In fact, this technology has enabled the development of cells with conversion efficiencies increasing from around 4.0 % to a current maximum of 26.7 % within just a few years, highlighting its potential as a cost-effective and high-performance alternative.

Perovskite is a type of mineral with a specific crystal structure of calcium titanate ($CaTiO_3$), but the term is often used to refer to a class of materials that have this same crystal structure [5]. Hybrid organic-inorganic perovskites are materials that can be described by the general formula ABX_3, where X is a monovalent halide anion (typically I^-, sometimes with a small fraction of Cl^- or Br^-), while A and B represent two cations; in particular, A is usually an organic cation ($CH_3NH_3^+$, $HC(NH_2)_2^{2+}$), while B is a divalent metal cation (such as Pb^{2+} or Sn^{2+}). Cation A, larger than B, forms the centre of the unit cell. Cation B forms the corners of the unit cell and the centre of an octahedron. The ionic radius of the cell plays a crucial role in the stability of the cubic unit cell

* Corresponding author.
E-mail address: salvatore.barreca@unict.it (S. Barreca).

https://doi.org/10.1016/j.jece.2025.118098
Received 26 April 2025; Received in revised form 9 June 2025; Accepted 14 July 2025
Available online 15 July 2025

[6,7].

Perovskite materials are a forefront research topic, given the unique combination of optoelectronic properties and solution processability. These characteristics have enabled perovskite solar cells (PSCs) to reach efficiencies higher than 27 %. Moreover, PSCs display enormous potential for modern unconventional Photovoltaic (PV) applications, since they can be made lightweight, semitransparent (ST), and/or flexible by means of appropriate design strategies.

The simplicity in the modifications of A and B cations and of the X halides makes perovskite materials excellent alternatives to obtain specific application properties. In particular, the size of the cations (A, B) or anion (X) has a crucial role in modulating the optical and electronic properties [8]. In the field of photovoltaic applications, several studies have investigated the impact of altering the size of ions to tune the bandgap of the perovskite absorber [9]. Organic-inorganic lead halide perovskites exhibit light absorption in the entire visible spectral region that can be perfectly modulated by tuning the band gap through cation and/or anionic exchange [10]. Perovskite materials exhibit ambipolar behaviour for the transport of charges (electrons and holes) [11]. Thanks to the adequate mobility of both p-type and n-type charge carriers, the hybrid perovskite can be inserted between layers of selective electron and hole transport, leading to different device architectures [11].

Despite the positive aspects, a major concern is emerging regarding the low stability of these systems compared to classic silicon solar cells. In fact, one of the major problems to be solved in the field of perovskite solar cells is that of humidity which makes perovskite materials unstable. A suitable encapsulation of the devices could minimize these problems. The degradation of metal halide perovskites, such as $CH_3NH_3PbI_3$, represents a significant challenge for the stability of solar cells. Several studies [7,12] suggest that the degradation processes may start with the formation of hydrated compounds on the surface of the material, which subsequently propagates into the film. Some hypotheses suggest that degradation occurs in two distinct phases and that it strictly depends on the presence of water as described in the literature [6,7,13].

To limit and overcome the problems related to the degradation of perovskites, several solutions have been proposed [14–16]. For example, the use of bromides has been suggested to strengthen the hydrogen bonds in the perovskite film between the cation $CH_3NH_3^+$ and the anion $[PbX_6]^{4-}$, thus avoiding the formation of hydrated compounds. Subsequent studies explored the use of thiocyanate ion instead of bromide [17], demonstrating that this modification prevents device degradation even at relative humidity levels of up to 70 % [18]. Another strategy to improve device stability involves the use of highly hydrophobic derivatives, such as fullerene [19] and pyrene [20] derivatives, which form compact self-assembled layers, thus preventing water inclusion and subsequent device degradation. Indeed, water and oxygen can also influence degradation by oxidizing organic material, especially in the presence of light. Perovskite degradation results in the formation of materials, such as PbI_2 (or $PbBr_2$), small amounts of metallic lead and carbonate compounds. Hydroiodic acid and methylamine can be formed by reaction with carbonic acid [21]. These reactions could give rise to the release of a significant quantity of lead, which tends to strongly adsorb onto soil particles, generally remaining in the top centimetres of the soil, that is, in the part that most affects crops. Furthermore, HI can acidify soils, promoting the dissolution and vertical migration of metal ions and halides, thus increasing the risk of contamination and posing potential public health risks. Some studies [22,23] report the use of organic molecules as protective agents to limit the pollutants release from solar cells caused by atmospheric agents such as hail, stress fractures resulting from dynamic/static loads (wind, snow, ice, etc.) or from the possible thermal or physical propagation of undetected microscopic defects. Module fractures can also occur at the attachment point of the solar cells due to faulty fixings. The release of soluble constituents in contact with water at different pH values [24,25] can be considered as one of the major routes that poses a potential environmental risk during reuse or uncontrolled disposal of waste materials [26]. On another hand, uncontrolled waste disposal must be considered a potential source of lead pollution from PSCs. The analysis of pollutants from new emerging matrices, in this case from electronic devices is a topic of fundamental importance in current environmental science.

Among the constituting metals of solar cells, Pb is of particular concern due to its high toxicity [27].

The toxicity of Pb ranks second on the priority list of toxic substances, respectively Agency for Toxic Substances and Disease Registry (ATSDR, 2015); [28]. Lead creates health disorders such as sleeplessness, tiredness, hear and weight loss. The International Agency for Research on Cancer classified inorganic lead as probably carcinogenic to humans (Group 2) in 2006 IARC, 2006) [29]. The environmental impacts and sustainability throughout the entire life cycle can be evaluated by using the Life Cycle Assessment (LCA), i.e a structured, comprehensive method for the assessment of a device by quantifying its material- and energy-flows and the associated emissions caused in the life cycle of goods and services. This method also allows to take into consideration some concerning aspects such as the costs of the synthesis of the compounds used, as well as their instability that may lead to the leaching of hazardous decomposition products and to short operational lifetimes, ultimately hindering their commercialization [30]. Indeed, a study conducted using the LCA [31] highlights the toxicity of some precursors and effects on the environment, in particular of lead that increases species mortality and growth inhibition of different species.

The control of lead leakage is currently the most critical aspect in PSCs sustainability.

Currently, there is a lack of proper treatment for photovoltaic devices that contain hazardous metals and their recovery [32] and, the intent of some researchers is to quantify metals of toxicological concern from leaching of waste materials in environmental matrices. For this purpose, leaching tests can be used to investigate the role of several organic or inorganic molecules in reducing the release of toxic elements into the environment.

Different analytical techniques (atomic adsorption spectroscopic, potentiometric, etc.) have been employed to quantify hazardous elements in environmental matrices [33,34] and the most versatile methods used are inductive coupled plasma atomic emission spectroscopy (ICP-AES) or inductive coupled plasma hyphenated with mass spectrometry (ICP-MS) [35]. However, these last ones require well equipped laboratories and highly trained personal for their application. On the other hand, electrochemical methods, especially voltametric ones, are very useful for determining trace elements in food [36] and in matrices of environmental [37] and technological interest. Hence, these techniques have been used to assess lead release from PSCs, also due to the rapidity of the method.

An important strategy to mitigate Pb pollution from a PSC is through the use of encapsulants, as reported already for self-healing polymers [38], which can reduce Pb leakage by more than 2 orders of magnitude compared with those based on UV-cured resins; another example is the use of transparent phosphonic acid films on a cover glass, which can prevent Pb leaching from encapsulated PSCs by up to 96 % compared to nonencapsulated ones [39].

However, the degradation of encapsulant materials in PSCs can significantly reduce their performance; in fact, when encapsulants degrade, they can negatively impact PSCs in several ways [40]. Encapsulant degradation may weaken adhesion at layer interfaces, leading to delamination of the solar cell layers or can give rise to colour changing (e.g., yellowing due to photodegradation), reducing light transmittance to the perovskite absorber [41].

In this context, an innovative approach to reduce lead spilling from PSCs into the environments, can be achieved by using insoluble molecules in HTL layer to reduce lead/water mixing.

Recently, to further enhance the photovoltaic performance and make stable PSCs, fluorine substituted organic materials are used. However, in the literature few data [42,43] are reported about the effect of these

types of molecules concerning lead leaching into the environment.

In this paper, a study was carried out on PSCs perovskite cells prepared following the classic planar n–i–p configuration [44] with a new material as Hole Transport Layer (HTL), i.e. three different perfluoroalkylated pyrene compounds, that should minimize the lead leakage without altering the cell performance. To this aim several cell modules were subjected to leaching test carried out following for the first time the UNI EN 12457–2 standard, and the leached lead was quantified by using the Anodic Stripping Voltammetry (ASV), ensuring very low quantification limits (lower the μgL^{-1}). Furthermore, to allow a straightforward analysis of the intrinsic Pb leaching behaviour, PSCs without encapsulation were used; in fact, if the device encapsulation fails an increased metal leakage is observed [37]. At the best of our knowledge, this study represents the first report on the evaluation of the effect of Perfluoroalkylated Pyrenes compounds in perovskite solar cells on the lead leakage.

2. Experimental

2.1. Materials

All chemicals were used as received without any further purification. Methylammonium iodide (CH3NH3I, 99.9 %) was purchased from Ossila. Lead chloride (PbCl2, 99.999 %) was obtained from Alfa Aesar. Titanium(IV)isopropoxide (99.999 %), molybdenum trioxide (MoO3, 99.97 %), 4-tert-butylpyridine (TBP, 96 %), lithium bis(trifluoromethylsulphonyl)imide, 2,20,7,70-tetrakis(N,N-di-*p*-methoxyphenylamine)-9,9-spirobi-fluorene (Spiro-OMeTAD) (99 % HPLC), chlorobenzene (CB, anhydrous, 99.8 %), acetonitrile (ACN, anhydrous, 99.8 %), N,N-dimethylformamide (DMF, anhydrous, 99.8 %), and isopropanol (IPA, anhydrous, 99.5 %) and Gold wire, 1.0 mm, (0.04in) (99.9985 %) were purchased from Sigma Aldrich and used as they are. Acetone, isopropanol, Ti(IV) isopropoxide, HCl, spiro-OMeTAD, chlorobenzene, 4-tert-butylpyridine (TBP), DMF, tris(2-(1H-pyrazol-1-yl)-4-tert-butylpyridine)cobalt (III) (FK-209), Litium bis(trifluoromethanesulphonyl)imide (Li-TFSI), isopropanol, MoO_3,and Poly-TetraFluoroEthylene (PTFE) filters (0.2 μm) were purchased from Merck. Methyl ammonium iodide was purchased at Dyesol and $PbCl_2$ from TCI Chemicals, whereas the leadstock solution (1000 mg/L was obtained by J.T. Baker. Gold wire, 1.0 mm, (0.04in) 99.9985 %was s purchased from Sigma Aldrich.

2.2. Sample preparation of methylammonium-lead-iodide $CH_3NH_3PbI_3$ (MAPI) based perovskite planar devices

To prepare the planar n–i–p PSCs schematically reported in Fig. 1, glass substrates covered by a layer of Fluorine Tin Oxide (FTO) or Indium Tin Oxide (ITO), furnished by GreatCell Solar (Australia) were cleaned by sonication in acetone and isopropanol for 15 min. and dried by anhydrous N_2. Then, the devices were exposed to ultraviolet-ozone treatment for 40 min. A slightly acidic precursor solution for the compact TiO_2 layer was prepared by adding 175 μL titanium(IV) isopropoxide to a mixture of 17.5 μL 2 M HCl and 2.5 mL isopropanol under vigorous stirring for 10 min at room temperature. The resulting solution was immediately filtered through a 0.2 μm PTFE syringe filter (Millipore) and deposited onto the substrates by spin-coating at 2000 rpm for 60 s. After deposition, the substrates were placed on a hot plate at 125 °C for 10 min and subsequently at 500 °C for 45 min in a muffle furnace. Perovskite samples were prepared by adding 398 mg of methylammonium iodide (MAI) and 237 mg of $PbCl_2$ in 1 mL of DMF. After filtration, the perovskite solution was deposited by spin coating at 4000 rpm for 45 s, inside a nitrogen-filled glovebox. The substrates were heat treated at 105 °C for 1.5 h. The hole transport materials were deposited on the devices using a solution consisting of 72.3 mg of Spiro-OMeTAD in 1 mL of chlorobenzene under doping conditions with 4-tert-butylpyridine (TBP) (29 μL), tris(2-(1H-pyrazol-1-yl)-4-tert-butylpyridine)cobalt(III) (FK-209) (10 μL), and Li-TFSI (17.5 μL) as additives. Additives were added for all hole carriers, Li-TFSI was prepared from a 1.8 M stock solution in acetonitrile, while FK-209 was prepared from a 0.25 M stock solution in acetonitrile. The final HTM solutions were spin-coated onto the perovskite layers at 4000 rpm for 45 s, inside a glovebox to avoid ambient exposure during deposition.

Before the deposition of the gold electrode, 5 nm layer of MoO_3 was deposited on the devices by thermal evaporation. The gold electrodes (15 nm) were deposited on the substrate by thermal evaporation of elemental gold wire obtaining spots using a shadow mask, under high vacuum conditions.

Other cells were prepared adding to HTL different perfluoroalkylated pyrene compounds, synthesized by following a literature protocol [45]. In this case, 0.25 mL of each perfluoroalkylated pyrene solution in dichloromethane was added to 0.75 mL of Spiro-OMeTAD solution. The resulting solution was stirred for about 24 h, then it was filtered and deposited on the slide by spin coating, similarly to what was done for the deposition of the perovskite active layer. In order to investigate the possible effect of perfluorinated chain, different perfluoroalkylated pyrene compounds with 4, 6 and 8 carbon atoms chains (Pyr-C_4F_9, Pyr-C_6F_{13} and Pyr-C_8F_{17}) were used.

Four different types of solar cells were made using different supports and compounds as schematic reported in Fig. 1.

a) Indium Tin Oxide/Titanium dioxide/Perovskite/Spiro-OMeTAD/molybdenum trioxide/gold

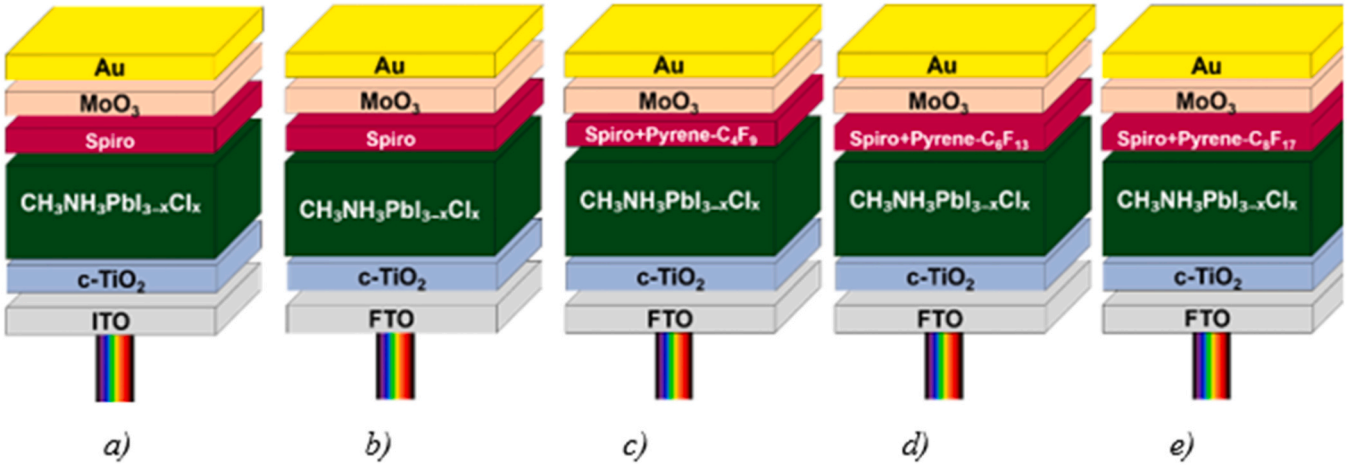

Fig. 1. Schematic representation of on-made photovoltaic module based on perovskite material.

b) Fluorine-doped tin oxide/Titanium dioxide/Perovskite/Spiro-OMeTAD/molybdenum trioxide/gold
c) Fluorine-doped tin oxide/Titanium dioxide/Perovskite/Spiro-OMeTAD+Pyrene functionalized with low CF chain/molybdenum trioxide/gold
d) Fluorine-doped tin oxide/Titanium dioxide/Perovskite/Spiro-OMeTAD+Pyrene functionalized with medium CF chain/molybdenum trioxide/gold
e) Fluorine-doped tin oxide/Titanium dioxide/Perovskite/Spiro-OMeTAD+Pyrene functionalized with long CF chain/molybdenum trioxide/gold

Investigated solar cells were made starting from a glass plate (100 mm×100 mm and thickness of 2.2 mm) and single modules were obtained by cutting the original glass sample into 2.5 × 2.5 cm (6.25 cm^2) pieces. Samples were stored under nitrogen, in dark condition and at room temperature until characterization and leaching investigations.

2.3. Solar cells characterization

Samples with (1e) or without (1b) perfluoroalkylated pyrene, were characterized for Power Conversion, calculated as percentage of incident solar power that is converted into electrical power following the Eq. 1:

$$PCE(\%) = \frac{Pout}{Pin} \quad x \quad 100 \tag{1}$$

where:

- Pout is the electrical power output (Voc×Jsc×FF)
- Pin is the incident solar power (typically 1000 W/m^2 under standard test conditions),
- Voc is the open-circuit voltage,
- Jsc is the short-circuit current density,
- FF is the fill factor.

The photovoltaic device performances were evaluated using a VeraSol LED solar simulator (Newport) producing 1 sun AM 1.5 G (100 W cm^{-2}) simulated sunlight. Current density-voltage curves (J/V) were measured in air with a potentiostat (Keithley). The light intensity was calibrated with an NREL certified KG5 filtered Si reference diode. The solar cells were masked with a metal aperture of 0.02 cm^2 to define the active area. The current-voltage curves were recorded scanning at 10 or 20 mV s^{-1}.

2.4. Leaching procedure

The leaching tests, performed in accordance with STANDARD UNI EN ISO 12457–2 procedure, i. e. under the tumbling condition for 24 h with a Liquid:Solid ratio10:1 at 20 °C, were made on materials with a grain size of at least 95 % (mass) less than 4 mm obtained from the crushing of different types of cells. The sample materials (5 g) were left in contact with 50 mL of different leaching agents for 24 h to simulate different environmental conditions. Deionized water, able to extract polar compounds, elements in ionic form, etc, was used. The solid residue was separated by filtration and the concentrations of Lead were measured using a modified voltammetric application method (Metrohm Application Work AW VA IT4–0003–052013) internally validated, as reported in quality control and quality assurance section. The fluorescence spectra on the leaching solutions were carried out on a Spectrofluorometer JASCO FP8200 by using a cell with an optical path of 1 cm.

2.5. Analytical method

For the quantitative determination of lead in the solutions obtained by the leaching procedure a computerized voltameter (AMEL model 4310) armed of a mercury film deposited for 30 s at −1200 mV on glassy carbon by a $HgCl_2$ solution (1000 mg/L) in HCl 6 M, an Ag/AgCl reference electrode in saturated KCl and a Pt counter electrode was used. For the quantification of lead, different accurately measured aliquots (50–2000 μL) of the solution obtained from leaching were added to appropriate milli Q water of a $HgCl_2$ solution (800 mg/L) in HCl 6 M, brought to a volume of 20 mL with Milli Q water and transferred to the voltammetric cell. Before signal acquisition, the dissolved O_2 was excluded by a N_2 flow, keeping the system under stirring. The quantitative measurements were performed using the standard addition procedure.

All the metal standard working solutions were daily prepared by dilution of a certified stock solution (1 mg mL^{-1}). Each standard addition generally gives rise to an increase in the solution concentration of 2 ppb. The operating parameters are reported in Table 1.

To detect possible leakage of perfluoroalkylated pyrene compound, a FP-8200 Spectrofluorometer was used.

2.6. Quality control and quality assurance

In order to assess the goodness of the developed method, blank solutions containing the same concentrations of chemicals used for the leaching tests, were investigated. For lead the mean value of the concentration in the blank solutions was < 2 ppb with a relative standard deviation about 3 %. Thus, the concentrations in the analysed samples were corrected for blank contribution, as suggested in literature [46].

The detection limit (LOD) and quantification limit (LOQ), were calculated as described in previous papers [33,46–49], as three- and ten-fold standard deviation of concentrations found in 7 procedural blanks, respectively. Repeatability was obtained by carrying out the analyses three times on the same sample (RSD % from 3 % to 10 %), while the method reproducibility was calculated as the relative standard deviation (RSD %) of independent analyses performed on three different leachates obtained from identical devices (RSD % values ranging from 10 % to 30 %). Good determination coefficient (R^2= 0.998) were obtained between the voltammetric peak current and the metal concentrations. The Trueness was also evaluated by using a spiked sample fortified at 10 ppb. Furthermore, the performances of the analyses were checked by using a second source standard in accordance with UNI EN ISO 17025. LOD, LOQ, analyses repeatability, method reproducibility and accuracy values are reported in Table 2.

3. Results

3.1. HTL structural characterization

To investigate how perfluoroalkylated pyrene compounds influence the morphology of the HTL, atomic force microscopies (AFM) investigation were performed both on Fluorine-doped tin oxide/Titanium dioxide/Perovskite/Spiro-OMeTAD/molybdenum trioxide/gold device used as classic Perovskite solar cells, and Fluorine-doped tin oxide/

Table 1
Operating parameters for the quantification of Lead.

Parameter	Pb^{2+}
Deposition Time (s)	60
Deposition Potential (mV)	−800
Scan Speed (mV/sec)	30
Number of Cycles	1
Delay Before Sweep (s)	5
Purge and Stir Time (s)	300
Stirring Speed (r.p.m)	300

Table 2
Validation parameters for lead analysis in leaching solutions.

	LOD	LOQ	S_r	S_R	Trueness	R^2
Pb^{2+}	0.5 ng L^{-1}	2 ng L^{-1}	10 %	30 %	70–130 %	0.998

Titanium dioxide/Perovskite/Spiro-OMeTAD+Pyrene-C_8F_{17}/molybdenum trioxide/gold and the images are shown in Fig. 2.

The reference sample exhibited higher surface roughness at the nanometer scale, with a root mean square (RMS) value of 9.95 nm over a 9 μm^2 area. In contrast, the sample doped with the pyrene-C_8F_{17} compound displayed a more uniform surface, with a roughness of 7.77 nm over the same area. The minimally altered or slightly smoother morphology suggests that the spiro-OMeTAD film remained structurally stable upon pyrene-C_8F_{17} compound incorporation.

Zhou et al. [50] suggest that the pinholes observed in the reference sample fully cover the surface layer, contributing to an increased RMS roughness. Likely, these aggregates result from the hydrolysis and aggregation of lithium salt (LiTFSI), a commonly used spiro-OMeTAD dopant. In fact, due to its hygroscopic nature, LiTFSI readily absorbs water and oxygen, promoting aggregates formation and layer degradation. However, introducing the perfluoroalkylated pyrene compound (Pyrene-C_8F_{17}) effectively mitigates moisture adsorption and prevents aggregation within the spiro-OMeTAD layer.

Although 4-tert-butylpyridine (TBP) is commonly added to spiro-OMeTAD to minimize LiTFSI phase segregation and ensure a homogeneous hole transport layer, its evaporation eventually leads to LiTFSI molecule aggregation. In fact, these standard dopants were observed to migrate toward the spiro-OMeTAD/anode (Au) interface due to their low affinity for the perovskite/HTL interface. Such morphological changes, driven by inhomogeneous doping, may negatively impact on the device stability, compromising the HTL/perovskite interface, hindering charge extraction and worsening its performances. Hence, the addition of perfluoroalkilated pyrene, which reduces the surface roughness, improves the stability of perovskite solar cells.

3.2. Power efficiency determination

In order to assess the role of perfluoroalkylated pyrene compounds in the HTL, the photovoltaic performances of solar cells 1b and 1e were evaluated by measuring the current vs the potential (see Fig. 3) and the corresponding calculated values are reported in Table 3. The two systems were selected by considering that solar cell 1b represents a standard photovoltaic solar cell, whereas in the HTL of cell 1e a perfluoroalkylated pyrene compound containing perfluoro octanoic acid (PFOA), one of the most investigated and used perfluorinated substances, was present.

Even if the introduction of pyrene compounds in the HTL has been reported as a factor enhancing the cell performance [51], the power conversion of cell 1e was found to be 20 % lower than that of cell 1b), but still comparable. Thus, the perfluoroalkylated pyrene compounds do not dramatically alter the power conversion of the devices and could be used in perovskite solar cells.

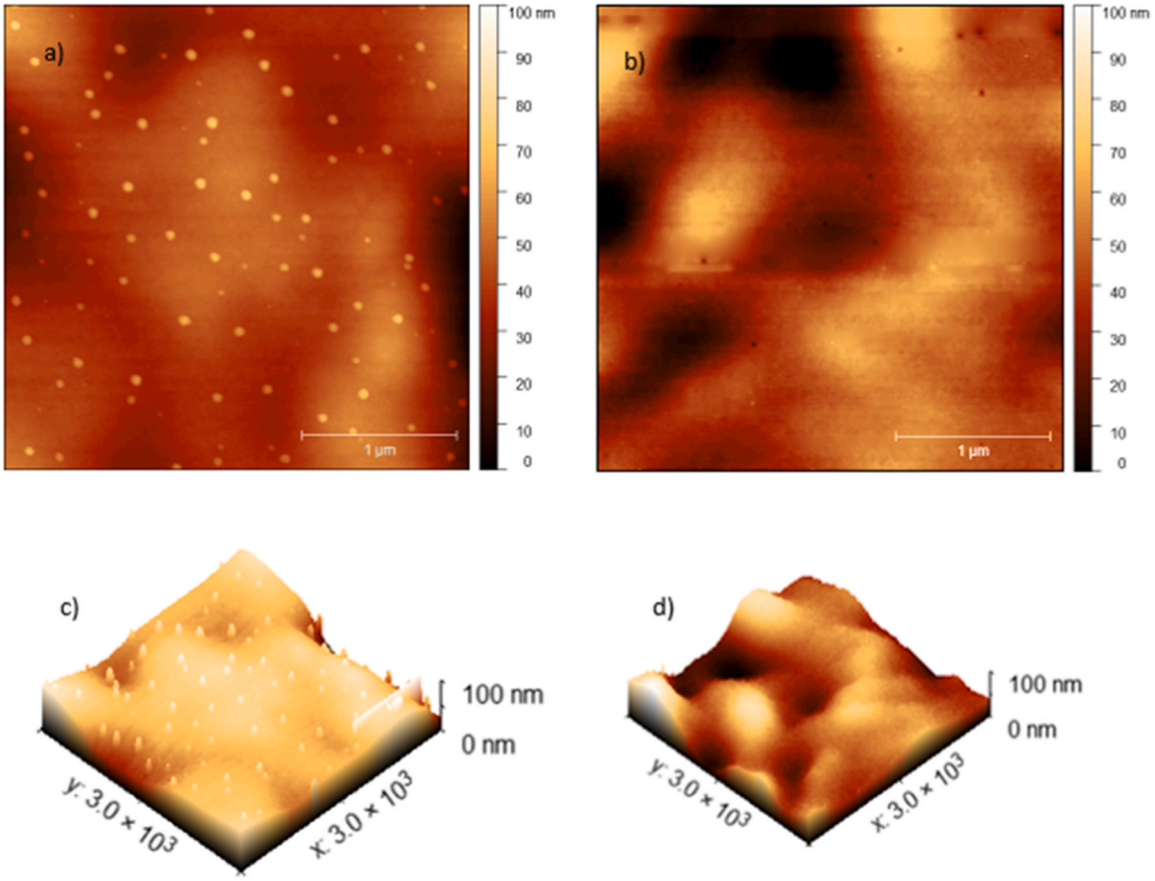

Fig. 2. Atomic Force Microscopies performed on devices a) Fluorine-doped tin oxide/Titanium dioxide/Perovskite/Spiro-OMeTAD/molybdenum trioxide/gold and b) Fluorine-doped tin oxide/Titanium dioxide/Perovskite/Spiro-OMeTAD+Pyrene-C_8F_{17}/molybdenum trioxide/gold. Surface roughness 3D maps c) of Fluorine-doped tin oxide/Titanium dioxide/Perovskite/Spiro-OMeTAD/molybdenum trioxide/gold and d) Fluorine-doped tin oxide/Titanium dioxide/Perovskite/Spiro-OMeTAD+Pyrene-C_8F_{17}/molybdenum trioxide/gold.

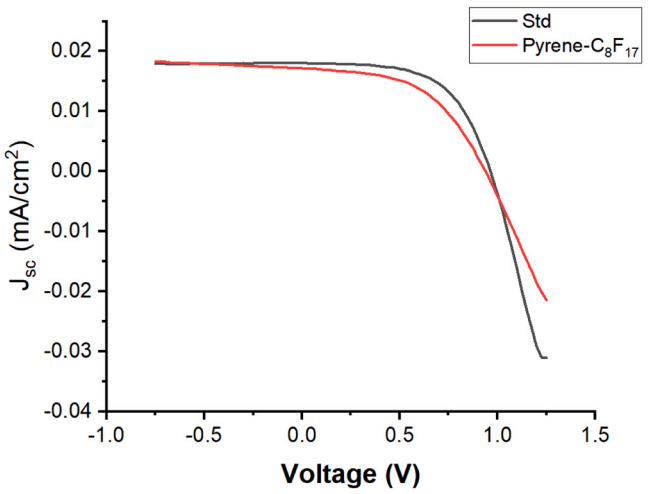

Fig. 3. J/V curves of devices (FTO/TiO_2/Perovskite/Spiro-OMeTAD /Au) (blu line) and 1c FTO/TiO_2/Perovskite/Spiro-OMeTAD+F537/Au (red line) under AM 1.5 G solar simulated illumination.

Table 3
Electrical parameters of the devices.

Sample	V_{oc} (V)	J_{sc} ($mAcm^{-2}$)	FF	PCE (%)
1b) FTO/TiO_2/Perovskite/Spiro-OMeTAD /Au	0.96	1.8	0.59	10.2
1e) FTO/TiO_2/Perovskite/Spiro-OMeTAD+C_8F_{17}/Au	0.96	1.7	0.50	8.3

3.3. *Leaching tests*

To investigate the effect of perfluoroalkylated pyrene compound on lead release, leaching tests were performed on the five different types of solar cells described in Fig. 1. The concentrations of lead leached out from perovskite solar cells extraction fluid, carried out as required from STANDARD UNI EN 12457–2, are reported in Table 4. The table shows that the highest concentration of lead leached was detected in the cell based on Indium Tin Oxide/Titanium dioxide/Perovskite/Spiro-OMeTAD/molybdenum trioxide/gold (12.8 mg/L) followed by solar cell type b) (Fluorine-doped tin oxide/Titanium dioxide/Perovskite/Spiro-OMeTAD/molybdenum trioxide/gold (5.5 mg/L)). This trend can be explained by the fact that ITO solar cells are lighter than those made in FTO; in fact, solar cells made in FTO are on average about twice as heavy as those made in ITO. Therefore, for solar cells with the same surface area, the concentration of Pb^{2+} ions present in the cell itself is higher in ITO cells than in FTO cells. Consequently, the release of lead into water is also higher, about twice as much.

The leaching tests data confirm that the standard perovskite solar cells can be considered as a possible source of lead contamination, taking into account the Lead Regulatory Limit of 5 mg/L [52].

Interestingly, the addition of perfluoroalkylated pyrene compounds in the HTL reduced the concentration of lead leached in solution below the Regulatory limit and therefore it is possible to conclude that the perfluorinated chains show an effect on lead leaching. In detail, lead leaching in solution decreased about 45 % in the case of perfluoroalkylated pyrene with C8 chain (see Fig. 4). In fact, fluorine is highly electronegative and when introduced into pyrene, it withdraws electron density from the π-system, lowering the highest occupied molecular orbital (HOMO) energy and widening the energy gap, affecting the charge transport properties. This effect was confirmed by taking into account the decrease in % PCE for the solar cells containing fluorinated pyrene.

On the other hand, the perfluorinated group or perfluoroalkyl chains are highly hydrophobic and thus can reduce the solubility of pyrene in water. Hence, the fluorinated pyrene molecules could act as a sort of barrier to water reducing the amount of lead that can be leached in solution. In conclusion, the HTL layer with fluorinated pyrene shows a slight decrease in solar cells performance but results in a significant decrease in the release of lead ions into solution. Fluorinated compounds have already been reported to increase the stability of solar cells [53].

Furthermore, the possible release of perfluoroalkyl pyrene compounds in solution was evaluated by recording the 3D fluorescence spectra of the leached solutions (see Supporting material S1).

Considering that pyrene in water can give fluorescent signals even at levels of 1 ppb [54] it can be stated that no release of perfluoroalkyl pyrene compounds above 1 ppb was observed, highlighting the good stability of these additives in the leaching tests.

In order to better understand the effect of the perfluoroalkyl chain length of perfluoroalkylated pyrene compounds on the release of lead into solution, the Pb^{2+} concentrations obtained by the release tests carried out on the cells containing different pyrene compounds with different chain lengths (Fig. 1c-e) were related to the n-octanol/water partitioning constants (K_{ow}) for analogous compounds containing a carboxylic group instead of pyrene and the results are shown in Fig. 5.

It is interesting to note that the length of the fluorinated chain did affect the release of lead into solution. In fact, as the length of the fluorinated chain increased, leading to a decrease in solubility and

Table 4
Concentrations of Lead leaching in solution obtained by following the UNI EN 12457–2 standard.

Solar Cell Types	Pb^{2+} mg/L in MilliQ water
ITO/TiO_2/Perovskite/Spiro-OMeTAD/Au	12.8
FTO/TiO_2/Perovskite/Spiro-OMeTAD/Au	5.5
FTO/TiO_2/Perovskite/Spiro-OMeTAD+F C_4F_9/Au	4.8
FTO/TiO_2/Perovskite/Spiro-OMeTAD+ C_6F_{13}/Au	3.6
FTO/TiO_2/Perovskite/Spiro-OMeTAD+C_8F_{17}/Au	3.0

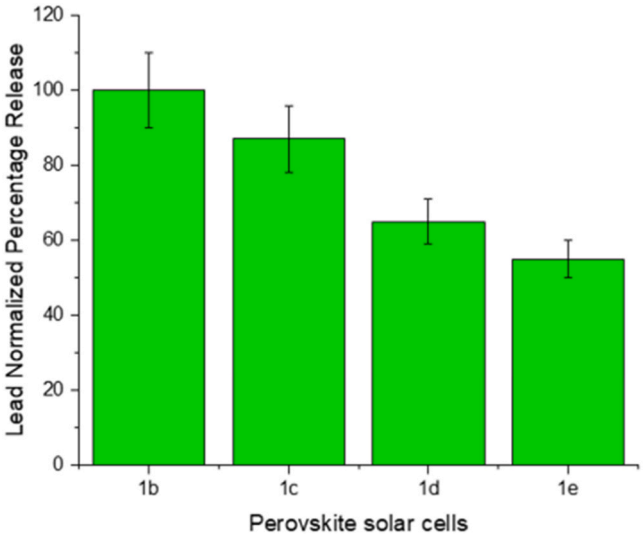

Fig. 4. Normalized percentages of lead released into the solutions obtained from leaching tests performed on different solar cells. 1b) Fluorine-doped tin oxide/Titanium dioxide/Perovskite/Spiro-OMeTAD/molybdenum trioxide/gold. 1c) Fluorine-doped tin oxide/Titanium dioxide/Perovskite/Spiro-OMeTAD+Pyrene functionalized with low CF chain/molybdenum trioxide/gold. 1d) Fluorine-doped tin oxide/Titanium dioxide/Perovskite/Spiro-OMeTAD+Pyrene functionalized with midium CF chain/molybdenum trioxide/gold. 1e) Fluorine-doped tin oxide/Titanium dioxide/Perovskite/Spiro-OMeTAD+Pyrene functionalized with long CF chain/molybdenum trioxide/gold.

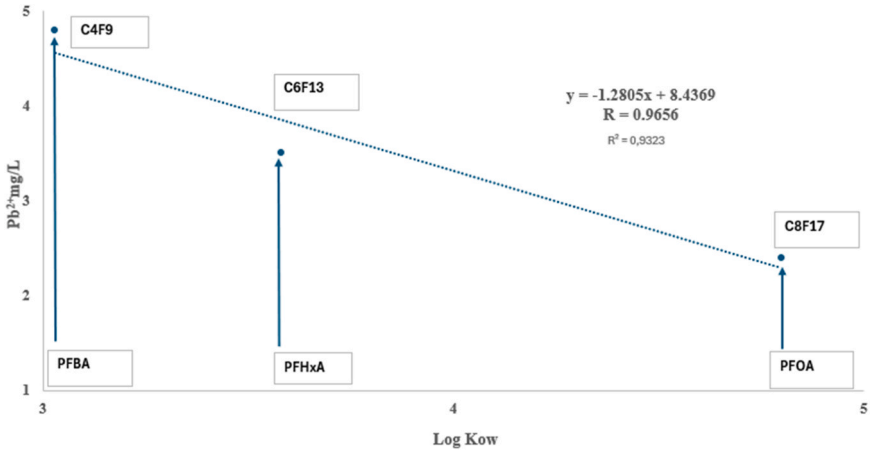

Fig. 5. Concentration values of lead in the leaching solutions as a function of the n-octanol/water partitioning constants (K_{ow}) for analogous compounds containing a carboxylic group instead of pyrene.

therefore to an increase in log K_{ow}, there was a decrease in the amount of lead released into solution. This trend shows a good determination coefficient with a value of $R^2 = 0.9323$.

3.4. Practical applications and future prospects

The use of perfluoroalkyl pyrene compounds in perovskite solar cells could be a good and practical strategy to limit lead leakage as well as to prevent the hydrolysis of lithium salts from these devices, increasing their stability over time and thus limiting their environmental impact. This could be a very promising strategy. In fact, these compounds, even if not commercially available, can be easily obtained by a fast and simple photochemical synthesis. Future perspectives could imply the combined use of perfluoroalkyl pyrene compounds and aromatic molecules to improve the cells efficiency, in order to obtain a new class of devices with better performances.

4. Conclusions

This study investigated the impact of perfluoroalkylated pyrene compounds on lead leaching from perovskite solar cells using, for the first time, standard UNI EN 12457–2.

The reported data show that the addition of perfluoroalkylated pyrene compounds in HTL of perovskite solar cells effectively mitigates lead ion migration by enhancing the film's morphological stability and reducing structural degradation. In fact, Atomic Force Microscopy analyses demonstrated a decrease in surface roughness in cells with pyrene compounds, suggesting improved film uniformity and reduced defect sites. Thus, by preventing lithium salt aggregation and phase separation within the hole transport layer, these additives contributed to the overall chemical stability of the device.

Furthermore, the hydrophobic nature of perfluoroalkylated pyrene compounds limited water penetration, a key factor in lead leaching. As a result, a reduced lead release was observed in perfluoroalkylated pyrene compounds doped samples, suggesting a promising pathway for improving the environmental and operational stability of perovskite-based photovoltaics. In detail, lead leaching in solution decreased about 45 % in the case of perfluoroalkylated pyrene with C8 chain, highlighting the good performances of this compound when used in perovskite solar cells to limit the environmental impact of these devices, due either to accidental breakage or when dismissed.

Long-term stability studies under standard conditions are essential to validate these findings and further develop strategies for lead containment in perovskite solar cells.

CRediT authorship contribution statement

Annalinda Contino: Writing – review & editing, Supervision, Writing – original draft. **Bruno Pignataro:** Writing – review & editing. **Davide Ricci:** Resources. **Giuseppe Maccarrone:** Writing – review & editing. **Giuseppe Arrabito:** Writing – review & editing, Project administration. **Santino Orecchio:** Writing – review & editing, Writing – original draft. **Alessandro Giuffrida:** Visualization. **Salvatore Barreca:** Writing – original draft, Conceptualization, Writing – review & editing, Funding acquisition. **Ivana Pibiri:** Resources. **Tiziana Fiore:** Resources. **Diana Amorello:** Data curation, Formal analysis. **Silvia Orecchio:** Formal analysis, Validation.

Ethical approval and consent to participate

This study did not involve human or animal participants.

Consent to publish

All authors have read and agreed to the published version of the manuscript.

Declaration of Competing Interest

The authors declare that they have no known competing financial interests or personal relationships that could have appeared to influence the work reported in this paper.

Acknowledgements

The research leading to these results has received funding from "ROBERTA-integrated Approach to Real Eco Sustainable Green Total Index" CUP E53D23015670001, project number P2022HEBEX funded by EU in Next Generation EU plan through the ITALIA "PRIN 2022 PNRR" finanziato dall'Unione Europea. AFM investigation were performed by Advanced Technologies Network (ATeN) Center (University of Palermo; project "Mediterranean Center for Human Health Advanced Biotechnologies (CHAB)", PON R&C 2007–2013) is also acknowledged for hospitality and service.

Appendix A. Supporting information

Supplementary data associated with this article can be found in the online version at doi:10.1016/j.jece.2025.118098.

Data availability

All data generated or analyzed during this study are with the authors, and, if necessary, they are available for taking any question about the datasets, which can be requested by reasonable request.

References

[1] T. Sharma, P.S. Chauhan, M. Patel, A. Singh, M. Kaur, G. Chauhan, B.B. Rana, N. Kumar, A. Walia, Carbon negative biofuels: a step ahead of carbon neutrality, Biofuels (2025) 1–21, https://doi.org/10.1080/17597269.2025.2450156.

[2] Ipcc. Global Warming of 1.5°C: IPCC Special Report on Impacts of Global Warming of 1.5°C above Pre-industrial Levels in Context of Strengthening Response to Climate Change, Sustainable Development, and Efforts to Eradicate Poverty, 1st ed, Cambridge University Press, 2022, https://doi.org/10.1017/9781009157940.

[3] S. Orecchio, D. Amorello, R. Indelicato, S. Barreca, S. Orecchio, A short review of simple analytical methods for the evaluation of PAHs and PAEs as indoor pollutants in house dust samples, Atmosphere 13 (2022) 1799, https://doi.org/10.3390/atmos13111799.

[4] A. Extance, The reality behind solar power's next star material, Nature 570 (2019) 429–432, https://doi.org/10.1038/d41586-019-01985-y.

[5] S. Thomas, A. Thankappan, Perovskite Photovoltaics: Basic to Advanced Concepts and Implementation, Academic Press, London, 2018.

[6] T.C. Birkett, Handbook of Mineralogy. IV. Arsenates, Phosphates, Vanadates.: By J. W. Anthony, R.A. Bideaux, K.W. Bladh and M.C. Nichols. Mineral Data Publishing, P.O. Box 37072, Tucson, Arizona 85740, U.S.A., or mineraldata.com, 2000, ix + 680 pages, $US108 plus $6 shipping and handling, hardbound (ISBN 0 9622097 0 8), Can. Miner. 38 (2000) 1487–1487, https://doi.org/10.2113/gscanmin.38.6.1487.

[7] Md.H. Miah, Md.B. Rahman, M. Nur-E-Alam, M.A. Islam, M. Shahinuzzaman, Md. R. Rahman, Md.H. Ullah, M.U. Khandaker, Key degradation mechanisms of perovskite solar cells and strategies for enhanced stability: issues and prospects, RSC Adv. 15 (2025) 628–654, https://doi.org/10.1039/D4RA07942F.

[8] J. Jean, P.R. Brown, R.L. Jaffe, T. Buonassisi, V. Bulović, Pathways for solar photovoltaics, Energy Environ. Sci. 8 (2015) 1200–1219, https://doi.org/10.1039/C4EE04073B.

[9] C.C. Stoumpos, M.G. Kanatzidis, The renaissance of halide perovskites and their evolution as emerging semiconductors, Acc. Chem. Res. 48 (2015) 2791–2802, https://doi.org/10.1021/acs.accounts.5b00229.

[10] L. Zheng, Y. Ma, S. Chu, S. Wang, B. Qu, L. Xiao, Z. Chen, Q. Gong, Z. Wu, X. Hou, Improved light absorption and charge transport for perovskite solar cells with rough interfaces by sequential deposition, Nanoscale 6 (2014) 8171–8176, https://doi.org/10.1039/C4NR01141D.

[11] F. Li, C. Ma, H. Wang, W. Hu, W. Yu, A.D. Sheikh, T. Wu, Ambipolar solution-processed hybrid perovskite phototransistors, Nat. Commun. 6 (2015) 8238, https://doi.org/10.1038/ncomms9238.

[12] D. Zhang, D. Li, Y. Hu, A. Mei, H. Han, Degradation pathways in perovskite solar cells and how to meet international standards, Commun. Mater. 3 (2022) 58, https://doi.org/10.1038/s43246-022-00281-z.

[13] E. Castro, J. Murillo, O. Fernandez-Delgado, L. Echegoyen, Progress in fullerene-based hybrid perovskite solar cells, J. Mater. Chem. C. 6 (2018) 2635–2651, https://doi.org/10.1039/C7TC04302C.

[14] O.J. Allen, J. Kang, S. Qian, J.J. Hinsch, L. Zhang, Y. Wang, A theoretical review of passivation technologies in perovskite solar cells, Energy Mater. 4 (2024), https://doi.org/10.20517/energymater.2023.111.

[15] S. Kulkarni, S. Gupta, J.V. Gohel, Contemporary neoteric energy materials to enhance efficiency and stability of perovskite solar cells: a review, J. Solid State Electrochem 28 (2024) 3051–3076, https://doi.org/10.1007/s10008-024-05905-7.

[16] Y. Zhang, J. Xi, Y. Deng, W. Liu, Z. Li, C. Liu, W. Guo, The crucial role of organic ligands on 2D/3D perovskite solar cells: a comprehensive review, Adv. Energy Mater. 14 (2024) 2403326, https://doi.org/10.1002/aenm.202403326.

[17] P.-Y. Lin, C.-F. Lin, Y.-Y. Chiu, H.-H. Chen, M.-H. Li, R. Raja, C.-S. Wu, C.-H. Hou, S. Sung-Yun Hsiao, J.-J. Shyue, D.-C. Lee, S.-Z. Ho, Y.-C. Chen, P. Chen, Revealing the role of thiocyanate for improving the performance of perovskite solar cells, ACS Appl. Energy Mater. 6 (2023) 79–88, https://doi.org/10.1021/acsaem.2c02291.

[18] P. Lin, A. Loganathan, I. Raifuku, M. Li, Y. Chiu, S. Chang, A. Fakharuddin, C. Lin, T. Guo, L. Schmidt-Mende, P. Chen, Pseudo-halide perovskite solar cells, Adv. Energy Mater. 11 (2021) 2100818, https://doi.org/10.1002/aenm.202100818.

[19] H. Wang, Z. Zhang, C. Zhang, Y. Yao, K. Wang, Structural modification of fullerene derivates for high-performance inverted perovskite solar cells, J. Mater. Chem. A 12 (2024) 22442–22457, https://doi.org/10.1039/D4TA03900A.

[20] K. Radhakrishna, S.B. Manjunath, D. Devadiga, R. Chetri, A.T. Nagaraja, Review on carbazole-based hole transporting materials for perovskite solar cell, ACS Appl. Energy Mater. 6 (2023) 3635–3664, https://doi.org/10.1021/acsaem.2c03025.

[21] C.A.R. Perini, A. Reddy Pininti, S. Martani, P. Topolovsek, A. Perego, D. Cortecchia, A. Petrozza, M. Caironi, Humidity-robust scalable metal halide perovskite film deposition for photovoltaic applications, J. Mater. Chem. A 8 (2020) 25283–25289, https://doi.org/10.1039/D0TA05003B.

[22] K. Manda, V.D. Jadhav, P. Chetti, R. Gundla, S. Pola, Molecular engineering of oxadiazole-based small organic-functional molecules as hole transporting materials for dopant-free perovskite solar cells, Org. Electron 136 (2025) 107153, https://doi.org/10.1016/j.orgel.2024.107153.

[23] R. Xing, Z. Li, W. Zhao, D. Wang, R. Xie, Y. Chen, L. Wu, X. Fang, Waterproof and flexible perovskite photodetector enabled by P-type organic molecular rubrene with high moisture and mechanical stability, Adv. Mater. 36 (2024) 2310248, https://doi.org/10.1002/adma.202310248.

[24] B. Hailegnaw, S. Kirmayer, E. Edri, G. Hodes, D. Cahen, Rain on methylammonium lead iodide based perovskites: possible environmental effects of perovskite solar cells, J. Phys. Chem. Lett. 6 (2015) 1543–1547, https://doi.org/10.1021/acs.jpclett.5b00504.

[25] Nikolskaia, A., Kozlov, S., Alexeeva, O., Vildanova, M., Karyagina, O., Almjasheva, O., Gusarov, V., Shevaleevskiy, O., 2023. NeW Inorganic Materials for Electron Transport Layers in Perovskite Solar Cells. https://doi.org/10.18721/JPM.161.172.

[26] G. Hu, Z. Li, Q. Zou, S. Zhou, S. Liang, L. Huang, H. Duan, J. Hu, H. Hou, L. Xu, C. Chen, J. Tang, J. Yang, Facile recovery of lead in discarded perovskite solar cells via ultrasonic water leaching, Environ. Sci. Technol. Lett. (2025) acs.estlett.4c00735, https://doi.org/10.1021/acs.estlett.4c00735.

[27] B.P. Lanphear, S. Rauch, P. Auinger, R.W. Allen, R.W. Hornung, Low-level lead exposure and mortality in US adults: a population-based cohort study, Lancet Public Health 3 (2018) e177–e184, https://doi.org/10.1016/S2468-2667(18)30025-2.

[28] Registry A A f T S a D Priority List of Hazardous Substances. https://www.atsdr.cdc.gov/programs/substance-priority-list.html.

[29] International Agency for Research on Cancer (Ed.), 2006. Inorganic and organic lead compounds: this publication represents the views and expert opinions of an IARC Working Group on the Evaluation of Carcinogenic Risks to Humans, which met in Lyon, 10 - 17 February 2004, IARC monographs on the evaluation of carcinogenic risks to humans. IARC, Lyon.

[30] M. Nur-E-Alam, M.S. Islam, T. Abedin, M.A. Islam, B.K. Yap, T.S. Kiong, N. Das, M. R. Rahman, M.U. Khandaker, Current scenario and future trends on stability issues of perovskite solar cells: A mini review, Curr. Opin. Colloid Interface Sci. 76 (2025) 101895, https://doi.org/10.1016/j.cocis.2025.101895.

[31] W. Akram, X. Li, S. Ahmed, Z. Ouyang, G. Li, A review of life cycle assessment and sustainability analysis of perovskite/Si tandem solar cells, RSC Sustain 3 (2025) 21–36, https://doi.org/10.1039/D4SU00431K.

[32] S. Murugapoopathi, R. Sathiyamoorthi, S. Senthil, Critical review on various recycling methods of indium from flat panel displays. in: Metal Value Recovery from Industrial Waste Using Advanced Physicochemical Treatment Technologies, Elsevier, 2025, pp. 261–276, https://doi.org/10.1016/B978-0-443-21884-2.00015-0.

[33] S. Barreca, S Orecchio, S. Orecchio, I. Abbate, C. Pellerito, Macro and micro elements in traditional meals of Mediterranean diet: determination, estimated intake by population, risk assessment and chemometric analysis, J. Food Compos. Anal. 123 (2023) 105541, https://doi.org/10.1016/j.jfca.2023.105541.

[34] F. Di Gaudio, D. Amorello, M. Ferrara, S. Orecchio, S. Orecchio, Heavy metals in tattoo inks: developing an analytical methodology for accessing customer safety, ChemistrySelect 8 (2023) e202300986, https://doi.org/10.1002/slct.202300986.

[35] K. Pitzke, K. Timm, R. Hebisch, T.H. Brock, A. Hartwig, M.A.K. Commission, Indium – Determination of indium and its compounds in workplace air using mass spectrometry with inductively coupled plasma (ICP-MS): Air Monitoring Method, Transl. Ger. Version 2021 (2021), https://doi.org/10.34865/AM744074E6_2OR.

[36] D. Amorello, S. Orecchio, Quantification of platinum in edible mushrooms using voltammetric techniques, Pollutants 1 (2021) 270–277, https://doi.org/10.3390/pollutants1040021.

[37] D. Yan, X. Lu, S. Zhao, Z. Zhang, M. Lu, J. Feng, J. Zhang, K. Spencer, T. Watson, M. Li, B. Hou, F. Wang, Z. Li, Lead leaching of perovskite solar cells in aqueous environments: a quantitative investigation, Sol. RRL 6 (2022) 2200332, https://doi.org/10.1002/solr.202200332.

[38] F. Liang, E. Akman, S. Aftab, M.K.A. Mohammed, H.H. Hegazy, X. Zhang, F. Zhang, Self-healing polymers in rigid and flexible perovskite photovoltaics, InfoMat 7 (2025) e12628, https://doi.org/10.1002/inf2.12628.

[39] R.D. Mendez L., B.N. Breen, D. Cahen, Lead sequestration from halide perovskite solar cells with a low-cost thiol-containing encapsulant, ACS Appl. Mater. Interfaces 14 (2022) 29766–29772, https://doi.org/10.1021/acsami.2c05074.

[40] R. Meena, A. Pareek, R. Gupta, A comprehensive Review on interfacial delamination in photovoltaic modules, Renew. Sustain. Energy Rev. 189 (2024) 113944, https://doi.org/10.1016/j.rser.2023.113944.

[41] J.H. Wohlgemuth, M.D. Kempe, D.C. Miller, Discoloration of PV encapsulants, in: 2013. IEEE 39th Photovoltaic Specialists Conference (PVSC), Presented at the 2013 IEEE 39th Photovoltaic Specialists Conference (PVSC), IEEE, Tampa, FL, USA, 2013, pp. 3260–3265, https://doi.org/10.1109/PVSC.2013.6745147.

[42] K. Dong, L. Zhu, G. Yang, L. Zheng, Y. Wang, B. Zhang, J. Zhou, J. Bian, F. Zhang, S. Yu, S. Liu, M. Wang, J. Xiao, X. Guo, X. Jiang, Influence of F-containing materials on perovskite solar cells, ChemSusChem 17 (2024) e202400038, https://doi.org/10.1002/cssc.202400038.

[43] P. Su, Y. Liu, J. Zhang, C. Chen, B. Yang, C. Zhang, X. Zhao, Pb-based perovskite solar cells and the underlying pollution behind clean energy: dynamic leaching of toxic substances from discarded perovskite solar cells, J. Phys. Chem. Lett. 11 (2020) 2812–2817, https://doi.org/10.1021/acs.jpclett.0c00503.

[44] G. Giuliano, A. Bonasera, M. Scopelliti, D. Chillura Martino, T. Fiore, B. Pignataro, Boosting the performance of one-step solution-processed perovskite solar cells using a natural monoterpene alcohol as a green solvent additive, ACS Appl. Electron. Mater. 3 (2021) 1813–1825, https://doi.org/10.1021/acsaelm.1c00084.

[45] I. Pibiri, S. Buscemi, A. Palumbo Piccionello, M.L. Saladino, D. Chillura Martino, E. Caponetti, Photochemical synthesis of pyrene perfluoroalkyl derivatives and their embedding in a polymethylmethacrylate matrix: a spectroscopic and

structural study, J. Mater. Chem. C. 2 (2014) 7722–7730, https://doi.org/10.1039/C4TC01187B.
[46] D. Amorello, S. Barreca, F. Pensato, S. Orecchio, Potentiometric analysis of fluoride in commonly consumed beverages: method development, evaluation, and risk assessment, J. Food Compos. Anal. 137 (2025) 106836, https://doi.org/10.1016/j.jfca.2024.106836.
[47] D. Amorello, S. Barreca, E. Gulli, S. Orecchio, Platinum and rhodium in wine samples by using voltammetric techniques, Microchem. J. 130 (2017) 229–235, https://doi.org/10.1016/j.microc.2016.09.010.
[48] D. Amorello, S. Orecchio, Micro-determination of dithiocarbamates in pesticide formulations using voltammetry, Microchem. J. 110 (2013) 334–339, https://doi.org/10.1016/j.microc.2013.05.002.
[49] D. Amorello, S. Orecchio, S. Barreca, S. Orecchio, Voltammetry for monitoring platinum, palladium and rhodium in environmental and food matrices, ChemistrySelect 8 (2023) e202300200, https://doi.org/10.1002/slct.202300200.
[50] Q. Lou, G. Lou, H. Guo, T. Sun, C. Wang, G. Chai, X. Chen, G. Yang, Y. Guo, H. Zhou, Enhanced efficiency and stability of n-i-p perovskite solar cells by incorporation of fluorinated graphene in the Spiro-OMeTAD hole transport layer, Adv. Energy Mater. 12 (2022) 2201344, https://doi.org/10.1002/aenm.202201344.
[51] J.-Y. Shao, Y.-W. Zhong, Pyrene-cored hole-transporting materials for efficient and stable perovskite solar cells, Bull. Chem. Soc. Jpn. 94 (2021) 632–640, https://doi.org/10.1246/bcsj.20200331.
[52] World Health Organization (Ed.), 2022. Guidelines for drinking-water quality, Fourth edition incorporating the first and second addenda. ed. World Health Organization, Geneva.
[53] S. Valero, T. Soria, N. Marinova, J.L. Delgado, Efficient and stable perovskite solar cells based on perfluorinated polymers, Polym. Chem. 10 (2019) 5726–5736, https://doi.org/10.1039/C9PY00992B.
[54] S. Barreca, I.P. Oliveri, F. Lo Presti, V. Oliveri, S. Giannakis, N. Tuccitto, V. Spampinato, A. Auditore, An innovative “up-and-down” adsorption processes for pyrene removal from acid wastewater as new approach in water remediation, Sep. Purif. Technol. 348 (2024) 127516, https://doi.org/10.1016/j.seppur.2024.127516.